

# Investigating the Effect of Tuning the Metal Center in Complexes for Nonlinear Optical Application

Mamoona Jillani<sup>a</sup>, Nur 'Athirah<sup>a</sup>, Suhaila Sapari<sup>a</sup>, Fazira Ilyana Abdul Razak<sup>a,b\*</sup>

<sup>a</sup>Department of Chemistry, Faculty of Science, Universiti Teknologi Malaysia, 81310, UTM Johor Bahru, Johor, Malaysia; <sup>b</sup>Department of Chemistry, Faculty of Mathematics and Natural Sciences, Universitas Negeri Malang, Indonesia

**Abstract** In this study, the new transition metal complexes, ML with M = Zn (II), Ni (II), and Pd (II) based on the N,N'-Bis[O-(diphenylphosphino)benzylidene]ethylenediamine ligand were successfully synthesized with a percentage yield of between 33 – 68%. As a result of fourier transform infrared spectroscopy (FTIR), UV-vis spectroscopy (UV-vis), and <sup>1</sup>H nuclear magnetic resonance (proton NMR) was used to design and completely describe the metal complexes properties. Moreover, for computational study, the Gaussian16 software installed in the high-performance computer (HPC) is used for NLO calculation. The method used to perform this study is Density Functional Theory (DFT) method. 6-31G(d,p) basis set is used with LANL2DZ for zinc, nickel, and palladium along with the keyword 'GEN'. The molecular structure has been optimized and checked both bond length and bond angle before starting to run the calculation. Thus, NLO calculation had been performed. The dipole moment and the HOMO-LUMO energy gap were employed to verify the first hyperpolarizability,  $\beta_{tot}$ , which can be utilized as an indication of second nonlinear optical characteristics. Transition metal-based complexes produce impressive results because they provide additional flexibility by offering charge transfer (CT) transitions between the metal and the ligands, resulting in a higher NLO response. Due to the charge transfer excitations, it was discovered that the nickel complex with 2.87 D had the largest NLO response ( $117215.66 \times 10^{-30}$  esu), particularly in comparison with the zinc complex ( $2329.72 \times 10^{-30}$  esu) and palladium complex ( $191.07 \times 10^{-30}$  esu) with 6.52 D and 4.04 D values, respectively.

**Keywords:** Density functional theory, Nonlinear optic property, Nickel complex, Zinc complex.

## Introduction

Non-optics is the study of light's interactions with matter under situations in which the atoms' non-linear response is significant. Transition metal-based complexes produce impressive results because they provide additional flexibility by offering charge transfer (CT) transitions between the metal and the ligands, resulting in a higher NLO response. In recent decades, non-linear optics (NLO) has been a fast-rising scientific topic based on the phenomena of strong coherent light radiation interacting with the matter gaining a lot of attention for the application in data storage, signal processing, sensing and optoelectronic technology [1-2]. Major improvements in new technologies are frequently attributed to the introduction of the new materials of greater quality. Photonic technology upgradation is highly based on the improvements made in the modelling of the materials for novel optical devices that work better [3]. When powerful electromagnetic fields, such as those found in a laser beam, interact with the matter, the polarisation of single molecule changes its dipole moment because of its electrical reaction the distortion of spatial distribution between electrons and the nucleus causes the nonlinearity to occur [4]. Crystals or amorphous materials while interacting with high radiation photons are effective

\*For correspondence:

faziraillyana@utm.my

Received: 7 March 2023

Accepted: 21 Sept. 2023

©Copyright K. Jillani. This article is distributed under the terms of the [Creative Commons Attribution License](#), which permits unrestricted use and redistribution provided that the original author and source are credited.

in generating twice the frequency of initial photons to produce NLO effects are selectable in terms of large responses, rapid reaction times, manufacturing and incorporation into composites and freedom of designing. All these excellent qualities required for the NLO applications can be seen in organometallics with the variety of geometries. Mixed-metal systems can operate as donor or acceptor groups that can stabilise the framework. [5].

Multifunctional NLO materials can have both organic and inorganic framework but due to large polarization, conjugated structures, asymmetrical crystal packing and charge distribution organic metal-based systems have been consistently chosen as NLO materials. Furthermore, transition metal-based organic systems such as ruthenium, copper, iridium, titanium, and platinum provide a high charge transfer (CT) distribution and strong electron delocalisation effect resulting in higher NLO responses. Because of the nature of charge transfer excitations, NLO contrasts are predicted in these metal complexes [6-7]. Nonlinearity of a system can be enhanced by the addition of the metals to the ligands thus can resist high temperatures and pressures [8-9].

Researchers have also conducted extensive software studies on NLO properties, and it is critical to evaluate the efficacy and feasibility of various computational study methods for application in NLO research. Besides, the mechanism and structure-property relationship of the closed shell framework were investigated by the computational approach is still lacking [10-12]. For quantum chemical electronic structure computations, *ab initio* approaches, semiempirical methods, and density functional theory (DFT) methods 6-31G/B3LYP and LANL2DZ are commonly utilised, and they are all based on the Schrodinger wave equation [13-14]. In addition, for the investigation of NLO property via computational stimulation, dipole moment ( $\mu$ ) and hyperpolarizability ( $\beta$ ) are computed by CAM-B3LYP/6-31G(d, p) method [15].

The HOMO-LUMO energy gap has traditionally been crucial to comprehending a molecule's electrical transitions. However, the most recent discoveries show that this energy gap also has a sizable impact on a material's NLO behavior. The alignment of HOMO and LUMO levels can have a significant impact on a material's sensitivity to NLO effects. Researchers have been able to clarify the fundamental mechanisms driving the relationship between HOMO-LUMO properties and NLO responses thanks to cutting-edge experimental techniques and computational methods. These findings demonstrate the close relationship between energy levels, orbital symmetries, and the effectiveness of NLO processes. This knowledge has given engineers a road map for developing materials with improved NLO characteristics. Recent research has also demonstrated the potential for molecular engineering to control HOMO and LUMO levels, hence adjusting NLO behaviour.

In this study, the best metal that affect NLO application was valuable for the experimental examination of the compounds and for speeding up the experimental procedure. The most promising complex would be used as a prime contender with improved nonlinear optic properties. Thus, the effects of the new transition metal complexes ML with M = Zn (II), Ni (II), and Pd (II) based on the L= N,N'-Bis[O-(diphenylphosphino)benzylidene]ethylenediamine ligand on NLO application was investigated. Besides, for structure confirmation spectroscopy FTIR, UV-vis,  $^1\text{H}$  NMR and  $^{31}\text{P}$  spectra were used to characterize the metal complexes.

## Materials and Methods

The research work in this study was carried out in two different parts. The first part was the preparation for the synthesis complexation of ligand with metal chloride and the characterization of the complex. The characterization technique used to characterize the complex were FTIR-spectroscopy, UV-vis, and NMR spectroscopy. A systematic and consistent theoretical technique to analyse the zinc and nickel complex NMR has not published yet, however for palladium complex it is yet unexplored in the literature. Lastly, in the second part of the study was focuses on doing the computational work on NLO for the ruthenium complex. Geometry optimization was done on the compound studied using GEN hybrid with density functional theory (DFT) method. The LANL2DZ basis set was used for metal, while 6-31G was used for optimizing the ligand. Figure 1 shows the materials being investigated.

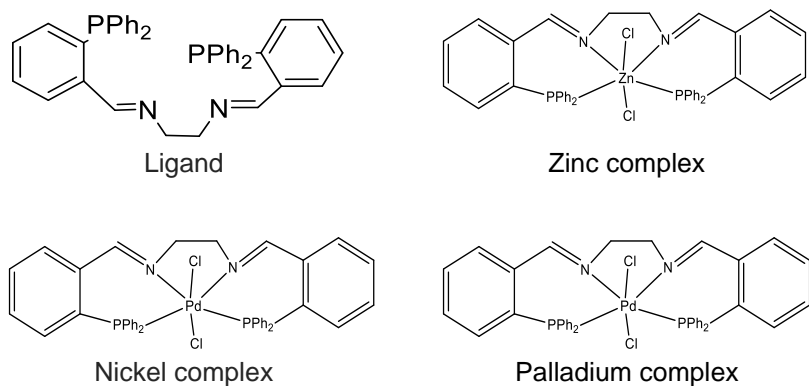


**Figure 1.** Studied Materials

All the chemical used in in this study purchased from Sigma Aldrich and Merck were used with no further purification included zinc chloride, palladium chloride, nickel chloride and the solvent used are dichloromethane, methanol, and ethanol. The nitrogen gas is used throughout the preparation of complexes to promote inert gas condition. Agilent Cary 630 FTIR spectrometer with a resolution of  $4.0\text{ cm}^{-1}$  was used to record the Fourier transform infrared (FTIR) spectrum of the solid investigated molecule. The produced sample was compacted into a self-supporting pellet and placed into a  $4000\text{--}400\text{ cm}^{-1}$  IR cell with a KBr pallet. The electronic absorption spectra of metal complexes were recorded on Shimadzu UV-1800 UV-vis spectrophotometer.  $^1\text{H}$  and  $^{31}\text{P}$  NMR spectra were recorded on Bruker Advance Spectrophotometer at 400 MHz NMR. The sample concentration should be at least 10.0 mg or 20.0 mg for  $^{31}\text{P}$  tests [3].

### Synthesis of N, N' -Bis-(2-diphenylphosphanyl-benzylidene)-ethane-1, 2-diamine dichloro zinc

Synthesis of zinc complex was carried out with the ligand and zinc chloride in solution. The procedure of the complex has been modified from the reported study [8] in terms of the starting materials, duration, and temperature of the reflux system. In a solution of N,N'-bis[o-(diphenylphosphino)benzylidene]ethylenediamine ( $\text{P}_2\text{N}_2$ ) (0.260 g, 0.395 mmol) in dichloromethane (20 ml) was added a solution of  $\text{ZnCl}_2$  (0.059 g, 0.433 mmol) (10 ml) in methanol drop wise with constant stirring. The reaction mixture was stirred for half an hour at room temperature before being refluxed for around 20 hours at  $70^\circ\text{C}$ . The product obtained is white solid with 0.054 g. The percentage yield of the product is 33 %.  $^1\text{H}$  NMR (400MHz,  $\text{CDCl}_3$ ),  $\delta$  [ppm]: 7.62 (-HC=N); 6.81-7.35 (ArH).  $^{31}\text{P}$  NMR,  $\text{CDCl}_3$ ,  $\delta$  [ppm]: 34.82. FTIR (KBr) ( $\text{cm}^{-1}$ ): 3141.27 m  $\nu$  (CH)ar, 1651.76 s  $\nu$  (C=N), 1624.42 s  $\nu$  (C=C)ar, 1453.42 m  $\nu$  (CH)  $\text{sp}^2$ .

### Synthesis of N, N' -Bis-(2-diphenylphosphanyl-benzylidene)-ethane-1, 2-diamine dichloro nickel

Synthesis of nickel complex has been done with the ligand and nickel chloride in solution. The procedure of the complex has been modified from the reported study [8] in terms of the starting materials, duration and temperature of the reflux system. In a solution of N,N'-bis[o-(diphenylphosphino)benzylidene]ethylenediamine ( $\text{P}_2\text{N}_2$ ) (0.1814 g, 0.300 mmol) in ethanol (10 ml) was added a solution of  $\text{NiCl}_2$  (0.0389 g, 0.300 mmol) (10 ml) in ethanol drop wise with constant stirring. The reaction mixture was stirred for half an hour at room temperature before being refluxed for around 20 hours at  $70^\circ\text{C}$ . The product obtained is light brown solid with 0.1417 g. The percentage yield of the product is 64 %.  $^1\text{H}$  NMR (400MHz,  $\text{CDCl}_3$ ),  $\delta$  [ppm]: 8.14 (-HC=N); 7.24-8.13 (ArH).  $^{31}\text{P}$  NMR,  $\text{CDCl}_3$ ,  $\delta$  [ppm]: 32.14. FTIR (KBr) ( $\text{cm}^{-1}$ ): 3211.04 m  $\nu$  (CH)ar, 1726.14 s  $\nu$  (C=N), 1632.03 s  $\nu$  (C=C)ar, 1435.23 m  $\nu$  (CH)  $\text{sp}^2$ .

### Synthesis of N, N' -Bis-(2-diphenylphosphanyl-benzylidene)-ethane-1, 2-diamine dichloro palladium

Synthesis of palladium complex has been done with the ligand and palladium chloride in solution. The

procedure of the complex has been modified from the reported study [8] in terms of the starting materials, duration, and temperature of the reflux system. In a solution of N,N'-bis[*o*-(diphenylphosphino)benzylidene]ethylenediamine (P<sub>2</sub>N<sub>2</sub>) (0.1814 g, 0.300 mmol) in ethanol (50 ml) was added a solution of PdCl<sub>2</sub> (0.0532 g, 0.300 mmol) (10 ml) in ethanol drop wise with constant stirring. The reaction mixture was stirred for half an hour at room temperature before being refluxed for around 20 hours at 60°C. The product obtained is dark brown solid with 0.1501 g. The percentage yield of the product is 68 %. <sup>1</sup>H

NMR (400MHz, CDCl<sub>3</sub>), δ [ppm]: 7.24-7.49 (ArH). FTIR (KBr) (cm<sup>-1</sup>): 3055.71 m ν(CH)<sub>ar</sub>, 1644.42 s ν(C=N), 1568.35 s ν(C=C)<sub>ar</sub>, 1436.83 m ν(CH)<sub>sp<sup>2</sup></sub>.

$$\text{Percentage deviation} = \frac{\text{Calculated value} - \text{Experimental value}}{\text{Experimental value}} \times 100 \%$$

## Computational Approach

For this study, computational work was carried out in the computer lab. Gaussian16 software which is installed in desktop was used for NLO calculation. The method used to perform this study was density functional theory (DFT) method. The basis set used in this method are 6-31G and LANL2DZ basis set. LANL2DZ is used for zinc, nickel, and palladium transition metal while 6-31G are used for another atom in the compound that employed for the 'GEN' keyword in Gaussian. The keyword combination used is "Pseudo=Read". Before starting to run the calculation, need to optimize the molecular structure, check the bond length, and bond angle of the structure. Then, NLO calculations are performed.

## Results and Discussion

This study was divided into two parts, the first part is about the synthesis of metal complexes which are then characterized. Hence, FT-IR, UV-vis, <sup>1</sup>H NMR and <sup>31</sup>P NMR spectra can be used to determine the structural properties of the compounds. The second part is related to the computational study of the three complexes which contain different metals. It was focused on the study of NLO properties of the three complexes by using the value of first hyperpolarizability, β<sub>tot</sub> as the indicator. The stretching FTIR of important functional group for all the complexes was compared with computational value calculation tabulated at Table 1.

**Table 1.** FT-IR frequency of complex studied.

| Complex   |               | Functional Group |              |                     |              |
|-----------|---------------|------------------|--------------|---------------------|--------------|
|           |               | C=N              | C-H Aromatic | C-H sp <sup>2</sup> | C=C Aromatic |
| Nickel    | Experimental  | 1726.14          | 3211.04      | 1435.23             | 1632.03      |
|           | Computational | 1737.48          | 3177.10      | 1388.12             | 1644.42      |
|           | % Deviation   | 0.65             | 1.07         | 3.29                | 0.76         |
| Zinc      | Experimental  | 1651.76          | 3141.27      | 1453.42             | 1651.76      |
|           | Computational | 1706.31          | 3192.33      | 1382.30             | 1624.42      |
|           | % Deviation   | 3.30             | 1.63         | 5.15                | 1.68         |
| Palladium | Experimental  | 1644.42          | 3055.71      | 1436.83             | 1568.35      |
|           | Computational | 1735.91          | 3228.27      | 1502.56             | 1626.90      |
|           | % Deviation   | 5.56             | 5.65         | 4.57                | 3.73         |

## Synthesis of Zinc Complex

Zinc complex has been synthesised and a white solid has been obtained. The IR for experimental spectrum of the zinc complex shows band at 1651.76 cm<sup>-1</sup>, which can be attributed to C=N stretching vibration. The calculated value for zinc complex shows band at 1706 cm<sup>-1</sup> (C=N) and 1382.30 cm<sup>-1</sup> (C-

H sp<sup>2</sup>). Thus, calculation of percentage deviation shows 3.30% (C=N) and 5.15% (C-H sp<sup>2</sup>). For the aromatic ring, the absorbance peak at 3141.27 cm<sup>-1</sup> for C-H aromatic and 1651.76 cm<sup>-1</sup> for C=C indicate that the aromatic ring is present in the compound. For the calculated value of C-H aromatic appear at 3192.33 cm<sup>-1</sup> and 1624.42 cm<sup>-1</sup> for C=C aromatic. The data for the percentage deviation (as mentioned above) of C-H aromatic is at 1.63% while C=C aromatic is 1.68%.

Moreover, the NMR spectrum of zinc complex with the proton resonance signal at 7.62 ppm,  $\nu(-CH=N)$  in the <sup>1</sup>H NMR spectrum, showing azomethine protons while the computational shows at 8.22 ppm that giving percentage deviation of 7.87 %. The C-H aromatic peak has been observed at the range 6.81 - 7.35 ppm (Figure 2). The calculated value of the C-H aromatic absorbs around 6.89 – 7.55 ppm. From the <sup>31</sup>P NMR of Figure 3, the appearance peak at 34.82 ppm indicates the phosphorus in the phosphine group.

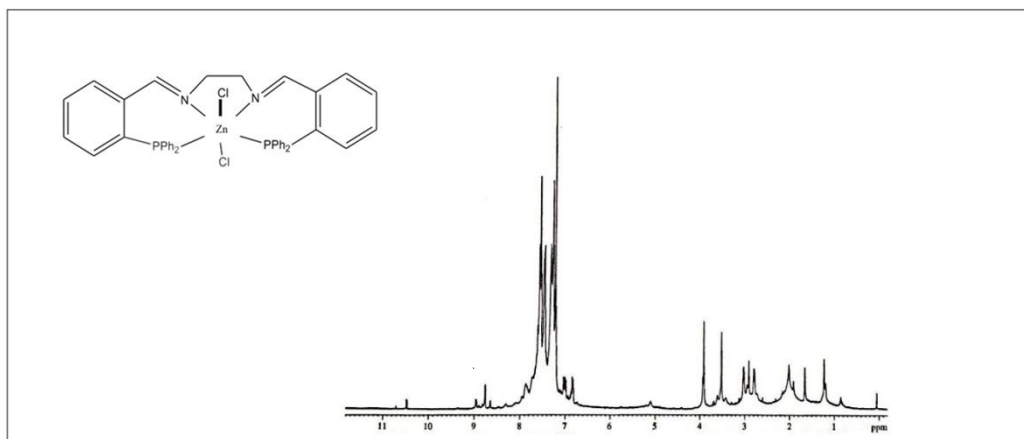


Figure 2. <sup>1</sup>H NMR spectrum for zinc complex

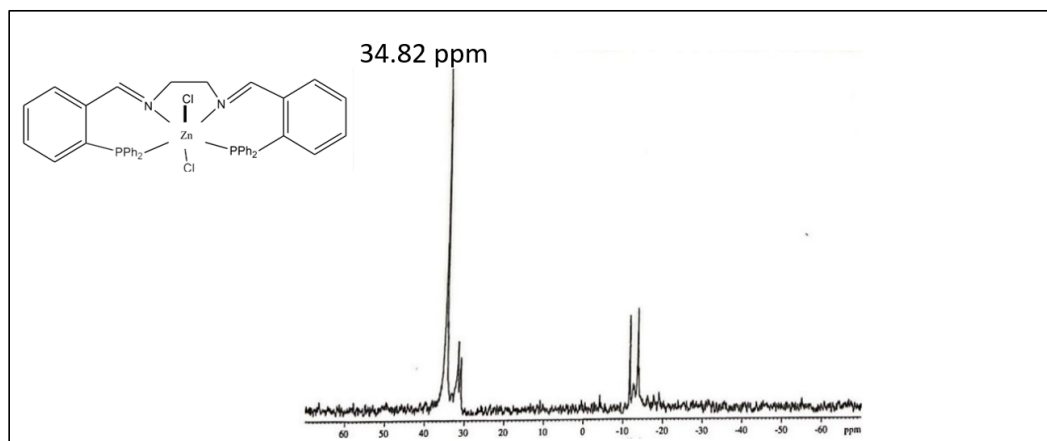


Figure 3. <sup>31</sup>P NMR spectrum for zinc complex

### Synthesis of Zinc Complex

Nickel complex has been synthesised and a light brown solid has been obtained. IR peak for this complex shows all the value of the percentage deviation below 5%. The experimental value of peak C=N is 1726.14 cm<sup>-1</sup> while the calculated value is at 1737.48 cm<sup>-1</sup> having percentage deviation of 0.65%. For C-H sp<sup>2</sup> peak, the experimental value absorbs at 1435.23 cm<sup>-1</sup> while 1388.12 cm<sup>-1</sup> is for the calculated value with percentage deviation of 3.29%. The experimental value for the C-H aromatic occurs at 3211 cm<sup>-1</sup> while calculated value is at 3177 cm<sup>-1</sup> having percentage deviation of 1.07%. C=C aromatic for experimental is at 1632 cm<sup>-1</sup> while calculated is at 1644 cm<sup>-1</sup> with the percentage deviation of 0.76%.

Furthermore, the spectrum of <sup>1</sup>H NMR of Figure 4 for the nickel complex shows the imine peak of 8.14 ppm and the C-H aromatic has absorbed at 7.24 – 8.13 ppm. While the analysis using <sup>31</sup>P NMR of Figure

5 shows that the appearance peak at 32.14 ppm indicates the phosphorus in the phosphine group. Unfortunately, there is no theoretical data from computational study to support the experimental spectra results as error occurred while dealing with the output file during the study.

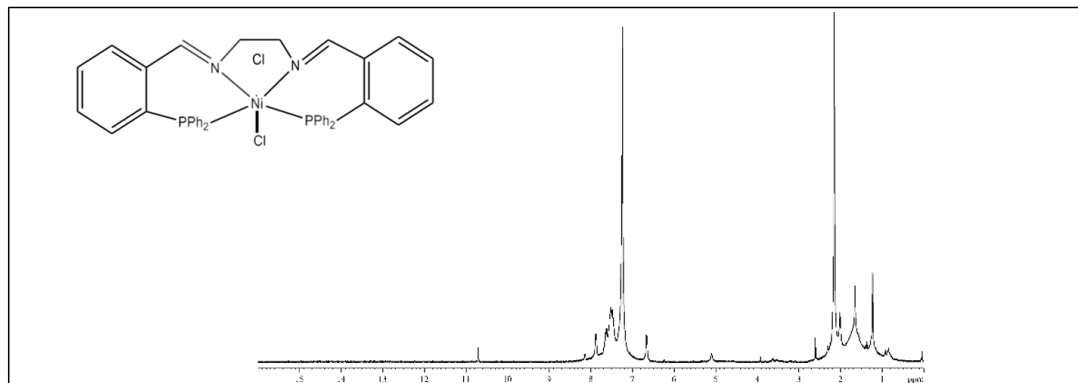


Figure 4.  $^1\text{H}$  NMR spectrum for nickel complex

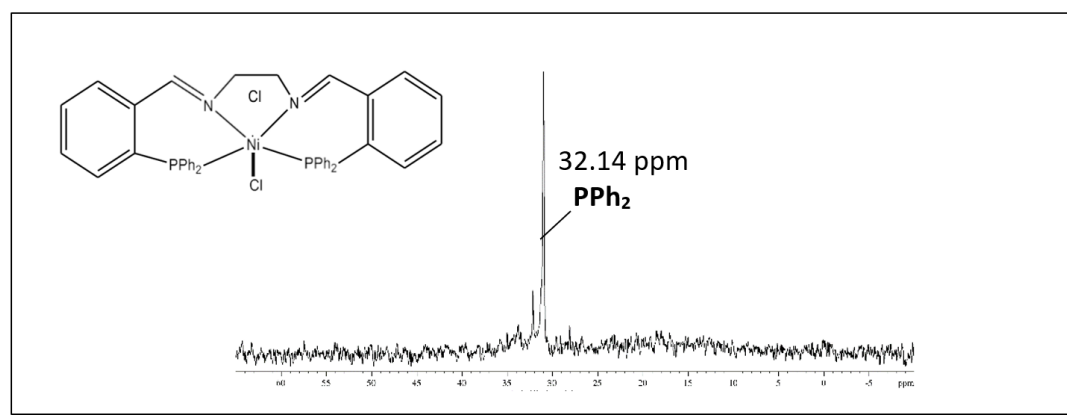


Figure 5.  $^{13}\text{C}$  NMR spectrum for nickel complex

### Synthesis of Palladium Complex

Palladium complex with dark brown solid has been obtained and IR peak for the C=C aromatic stretching is shown at  $1568.35\text{ cm}^{-1}$  while the calculated spectra is at  $1626.90\text{ cm}^{-1}$  with the percentage deviation of 3.73%. The experimental spectra for the C-H  $\text{sp}^2$  stretching have been absorbed at  $1436.83\text{ cm}^{-1}$  and the calculated spectra is at  $1502.56\text{ cm}^{-1}$  having the percentage deviation of 4.57%. The C=N vibration absorbed at  $1644.42\text{ cm}^{-1}$  for the experimental while the calculated spectra occur at  $1735.91\text{ cm}^{-1}$  with the percentage deviation of 5.56%. For CH aromatic stretching, the experimental value was absorbed at  $3055.71\text{ cm}^{-1}$  while  $3228.27\text{ cm}^{-1}$  for the calculated value with the percentage deviation of 5.65%. Percentage deviation less than 5 % proved the high accuracy of the basis sets used in optimizing the structure [16].

Hence, the  $^1\text{H}$  NMR spectral study further indicated the production of the palladium complex under investigation presented in Figure 6. For the C-H aromatic, the range value is at 7.24 – 7.49 ppm while the calculated value absorbs at 6.89- 7.70 ppm. However, the imine peak has not absorbed at spectrum while the calculated value shown at 8.32 ppm. For this palladium complex, the study of  $^{31}\text{P}$  NMR cannot be done because of the limited product.

Based on the observation, the products obtained are not pure as they are many noises peak of byproduct and probably containing starting materials as well. Therefore, further purification using column chromatography should be done.

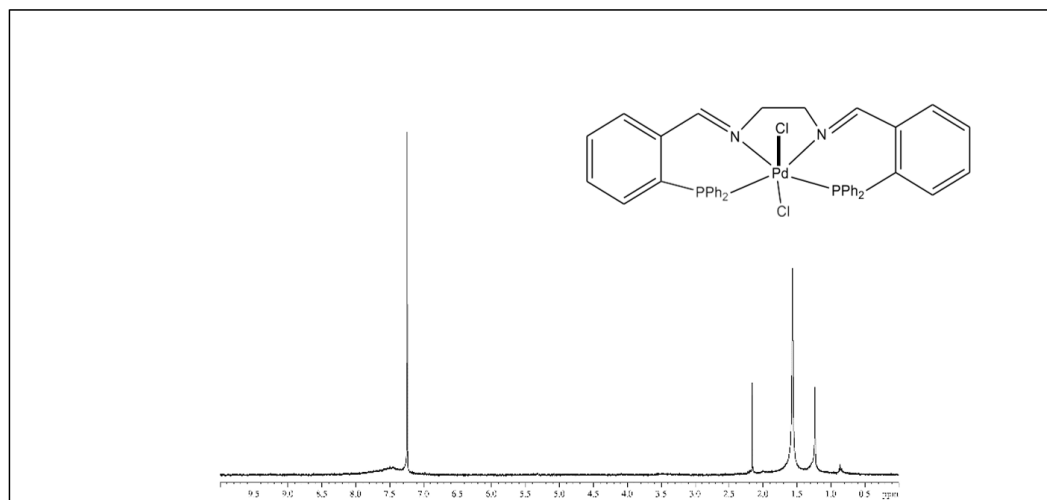


**Figure 6.**  $^1\text{H}$  NMR spectrum for palladium complex

### NLO Calculation

The calculation was done after the chemical was optimised by combining the "polar=gamma" term with "CPHF=RdFreq" in the task tab [17]. The computation was done using DFT approach at B3LYP/GENECP level [18]. The calculation for the frequency-dependent initial hyperpolarizability was done at 1064 nm, which is a commonly used laser frequency in NLO measurements [19]. Following the completion of the computation, the data was extracted, and the result was analysed. The total initial hyperpolarizability,  $\beta_{\text{tot}}$ , may be calculated using the formula below [20].

$$\beta_{\text{tot}} = (\beta_x^2 + \beta_y^2 + \beta_z^2)^{0.5}$$

$$\beta_x = \beta_{xxx} + \beta_{xyy} + \beta_{xzz}$$

$$\beta_y = \beta_{yyy} + \beta_{yxx} + \beta_{yzz}$$

$$\beta_z = \beta_{zxx} + \beta_{zyy} + \beta_{zzz}$$

Next the dipole moment of the studied complexes can be summarized in Table 2. Based on the result, zinc complex (6.5286 D) will have the higher dipole moment as compared to palladium complex (4.0450 D), whereas nickel complex (2.8736 D) is having the lowest dipole moment among the three complexes. The dipole moment in a molecule is generally due to the separation of charge and the difference of electronegativities in the structure. It is shown by molecule when it has a non-uniform distribution of positive and negative charges on itself.

Generally, as the value of  $E_{\text{gap}}$  decreases, the value of  $\beta_{\text{tot}}$  increases and the NLO properties increase. Also, because the HOMO-LUMO energy gap is smaller, greater charge is transferred inside the electron delocalization system, resulting in a high NLO characteristic [21].

**Table 2.** The energy, dipole moment and time of the compound studied.

| Compound          | Energy (a.u) | Dipole moment(D) | Time (s) |
|-------------------|--------------|------------------|----------|
| Zinc Complex      | -3323.0554   | 6.5286           | 69424    |
| Palladium Complex | -3384.1851   | 4.0450           | 115802   |
| Nickel Complex    | -3426.7327   | 2.8736           | 115464   |

When metal (zinc, nickel, or palladium) is combined with ligands that have various electron donating or withdrawing groups and distinct conjugated systems, the electronic structure and charge transfer alter,



resulting in variable NLO characteristics. The dipole moment and the HOMO-LUMO energy gap (Figure 7) may be used to verify the total first order hyperpolarizability,  $\beta_{\text{tot}}$ , which can be utilized as an indication of second nonlinear optic characteristics.

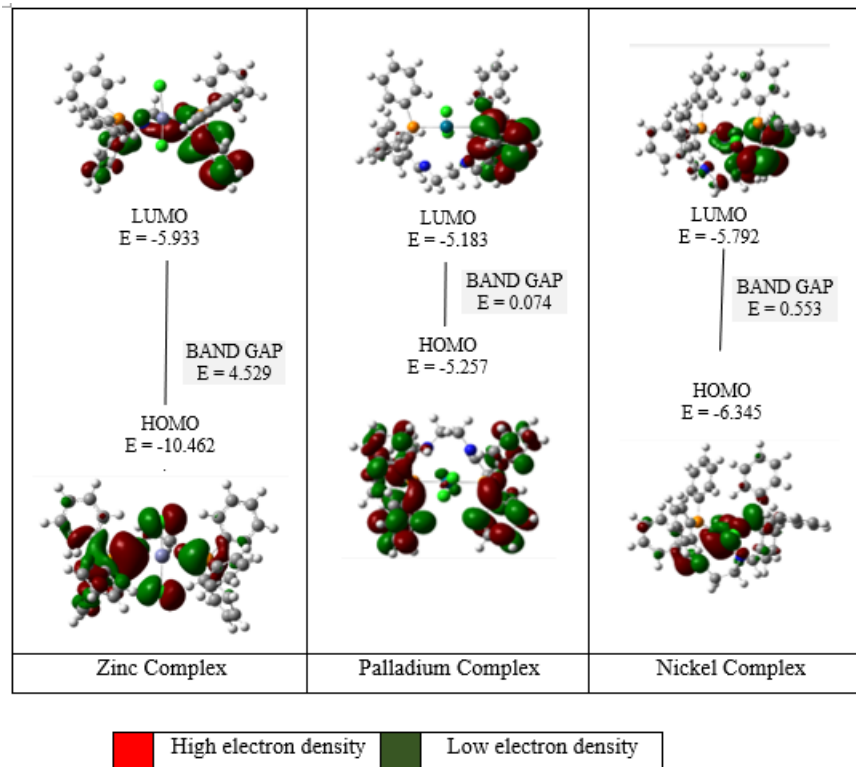


**Figure 7.** The HOMO and LUMO energy level of the studied compound

It was discovered in this research that the dipole moment cannot be used to estimate the NLO property. This is because the simulation of dipole moment is dependent on how the structure is sketched and calculated. Hence, the drawing structure should be symmetry also it is advisable to fix the drawing structure before proceeding the NLO calculation. Aside from that, the calculating approach utilized in this research does not include the diffusion impact. As a result, it will become one of the factors contributing to the lower accuracy of the outcome result.

In Table 3, it was found that the calculation of band gap shows a positive relationship in predicting NLO response. This study has shown that the NLO property can be related when having the lower band gap, will have higher NLO value. It can be illustrated from the data of nickel complex shows the lowest energy band gap (0.074 eV) than palladium (0.553 eV) and zinc complex (4.25 eV). This can present the efficient hopping of energy level from the lower state to the higher state. Thus, it could become a good candidate for another application such as bioactivity application.

Thus, nickel complex provides highest NLO at  $117215.66 \times 10^{-30}$  esu as compared to zinc complex at  $2329.72 \times 10^{-30}$  esu and palladium complex at  $1912.07 \times 10^{-30}$  esu. Besides that, from the highest value of NLO for Ni complex is because the situation known as "back-bonding" occurs when the cyanide donates its sigma (nonbonding) electrons to the metal while accepting electron density from the metal through overlap of a metal  $t_{2g}$  orbital and a ligand  $\pi^*$  orbital because the ligand donates  $\sigma$ -electron density to the metal and the metal donates  $\pi$ -electron density to the ligand. The ligand is then acting as a  $\sigma$ -donor and a  $\pi$ -acceptor [22]. The metal gives electrons to the ligand  $\pi^*$  orbital in  $\pi$ -back bonding, increasing electron density in an antibonding molecular orbital. Hence, the lowest number of electrons of nickel as compared to zinc and palladium as obviously showed in periodic table may affect the strength of the bond. Moreover, nickel has an empty d orbital as compared to full fill d orbital for zinc despite both metals have slightly differences number of electron.

It has been proved that the size and chemical properties of transition metal studied contribute to the enhancement of the NLO property.



**Table 3.** The energy, dipole moment and time of the compound studied

| Complex   | Dipole moment (D) | Band Gap (E) | NLO, $\beta$ ( $\times 10^{-30}$ esu) |
|-----------|-------------------|--------------|---------------------------------------|
| Zinc      | 6.5286            | 4.529        | 2329.72                               |
| Palladium | 4.0450            | 0.074        | 1912.07                               |
| Nickel    | 2.8736            | 0.553        | 117215.66                             |

## Conclusions

In conclusion, three different complexes were successfully synthesized, characterized, and optical and efficient NLO response qualities were studied. At the hybrid GEN/ DFT /6-31G\* level of theory, the microscopic NLO response characteristics were computed utilizing optimized molecular geometries of zinc (II) complex, nickel (II) complex and palladium (II) complex. Additionally, at the same level of theory, molecule geometry, dipole moments, polarizability, and molecular electrostatic potential (MEPs) maps were computed to get deeper physical insights into the structure property connection. The obtained results indicate that nickel (II) complex has good optical and NLO properties, which may render the above-entitled compounds as efficient candidates for optoelectronic and NLO device fabrication. Hence, we expect that the current discoveries will potentially boost the scientific community's interest in the synthesized compounds and their potential use in future optical and NLO research and applications.

## Conflicts of Interest

The author(s) declare(s) that there is no conflict of interest regarding the publication of this paper.

## Acknowledgment

The researcher would like to acknowledge the research grant support from Ministry of Higher Education, Malaysia for Fundamental Research Grant Scheme (FRGS, Vot R.J130000.7854.5F471). Faculty of Science UTM, and the Centre for Information and Communication Technology (CICT) for supporting and providing high-performance computing facilities and services to speed up the research. Thank you to the colleagues for the valuable support and suggestions.

## References

- [1] Baldwin, G. C. (2012). *An introduction to nonlinear optics*. Springer Science & Business Media.
- [2] Boyd, R. W., & Prato, D. (2008). *Nonlinear Optics*. USA: Elsevier Science.
- [3] Suresh, S., Ramanand, A., Jayaraman, D., & Mani, P. (2012). Review on theoretical aspect of nonlinear optics. *Reviews on Advanced Materials Science*, 30(2), 175-183.
- [4] Butet, J., Brevet, P.-F., & Martin, O. J. F. (2015). optical second harmonic generation in plasmonic nanostructures: From fundamental principles to advanced applications. *ACS Nano*, 9(11), 10545-105.
- [5] Green, K. A., Cifuentes, M. P., Samoc, M., & Humphrey, M. G. (2011). Metal alkynyl complexes as switchable NLO systems. *Coordination Chemistry Reviews*, 255(21), 2530-2541.
- [6] Bibi, T., Jadoon, T., Muhammad, S., & Ayub, K. (2021). Second order NLO properties and two-state switching effects of transition metal redox complexes of iron and cobalt: A DFT study. *Journal of Molecular Graphics and Modelling*, 107, 107975.
- [7] Anitha, C., Sumathi, S., Tharmaraj, P., & Sheela, C. (2012). Synthesis, characterization, and biological activity of some transition metal complexes derived from novel hydrazone azo schiff base ligand. *International Journal of Inorganic Chemistry*, 2011.
- [8] Chavan, S. S., Pawal, S. B., Lolage, S. R., & Garadkar, K. M. (2017). Synthesis, spectroscopic characterization, luminescence and NLO properties of heterometallic M(II)-Ru(II) (M=Ni and Zn) hybrid complexes composed of coordination and organometallic sites. *Journal of Organometallic Chemistry*, 853, 18-26.
- [9] Chavan, S. S., & Bharate, B. G. (2013). Heterobimetallic M(II)/Ru(II) (M=Ni, Zn) complexes containing coordination and organometallic sites: Synthesis, characterization, luminescence and NLO properties. *Inorganica Chimica Acta*, 394, 598-604.
- [10] Lind, P. (2007). *Organic and organometallic compounds for nonlinear absorption of light*. Kemi.
- [11] Comba, P., Hambley, T. W., & Martin, B. (2009). *Molecular modeling of inorganic compounds*. John Wiley &

- Sons.
- [12] Errol, G. L. (2011). *Computational Chemistry: Introduction to the theory and applications of molecular and quantum mechanics*. Springer, New York. 43, 44-45.
- [13] Perdew, J. P., & Yue, W. (1986). Accurate and simple density functional for the electronic exchange energy: Generalized gradient approximation. *Physical review B*, 33(12), 8800.
- [14] Siegbahn, P. E. (2006). The performance of hybrid DFT for mechanisms involving transition metal complexes in enzymes. *JBIC Journal of Biological Inorganic Chemistry*, 11(6), 695-701.
- [15] Lakshmi, C. S. N., Balachandran, S., Arul, D. D., Ronaldo, A. A., & Hubert, J. I. (2019). DFT analysis on spectral and NLO properties of (2E)-3-[4-(dimethylamino) phenyl]-1-(naphthalen-2-yl) prop-2-en-1-one; a d- $\pi$ -A chalcone derivative and its docking studies as a potent hepatoprotective agent.
- [16] Muscat, J., Swamy, V., & Harrison, N. M. (2002). First-principles calculations of the phase stability of TiO<sub>2</sub>. *Physical Review B*, 65(22), 224112.
- [17] Foresman, J., & Frisch, A. (2015). *Exploring Chemistry with Electronic Structure Methods*. 3rd edn., Wallingford, CT USA, Gaussian. In: Inc.
- [18] Mohamed, M. A., Mohd Hir, Z. A., Wan Mokhtar, W. N. A., & Osman, N. S. (2020). 6 - Features of metal oxide colloidal nanocrystal characterization. In S. Thomas, A. Tresa Sunny, & P. Velayudhan (Eds.). *Colloidal Metal Oxide Nanoparticles* (pp. 83-122): Elsevier.
- [19] Karakas, A., Dag, T., Taser, M., Fillaut, J., Migalska-Zalas, A., & Sahraoui, B. (2013). Second order hyperpolarizability and susceptibility calculations of a series of ruthenium complexes. Paper presented at the 2013 15th International. Conference on Transparent Optical Networks (ICTON).
- [20] Baseia, B., Osório, F. A., Lima, L. F., & Valverde, C. (2017). Effects of changing substituents on the non-linear optical properties of two coumarin derivatives. *Crystals*, 7(6), 158.
- [21] Khalid, M., Lodhi, H. M., Khan, M. U., & Imran, M. (2021). Structural parameter-modulated nonlinear optical amplitude of acceptor- $\pi$ -D- $\pi$ -donor-configured pyrene derivatives: A DFT approach. *RSC Advances*, 11(23), 14237-14250.
- [22] Cole, J. M., & Ashcroft, C. M. (2018). Generic classification scheme for second-order dipolar nonlinear optical organometallic complexes that exhibit second harmonic generation. *The Journal of Physical Chemistry A*, 123(3), 702-714.